The Molecular Basis of Vitamin E Retention: Structure of Human α-Tocopherol Transfer Protein

Article *in* Journal of Molecular Biology · September 2003

DOI: 10.1016/S0022-2836(03)00724-1 · Source: PubMed

5 authors, including:

Takashi Tomizaki

57 PUBLICATIONS **5,132** CITATIONS

SEE PROFILE

Clemens Schulze-Briese

DECTRIS LTd.

107 PUBLICATIONS **2,198** CITATIONS

SEE PROFILE

Achim Stocker

Universität Bern

73 PUBLICATIONS **1,973** CITATIONS

SEE PROFILE

doi:10.1016/S0022-2836(03)00724-1 J. Mol. Biol. (2003) 331, 725–734

JMB

Available online at www.sciencedirect.com

SCIENCE DIRECT®

The Molecular Basis of Vitamin E Retention: Structure of Human α-Tocopherol Transfer Protein

Reto Meier[1], Takashi Tomizaki[2], Clemens Schulze-Briese[2] Ulrich Baumann[1] and Achim Stocker[1]*

[1]*Department of Chemistry and Biochemistry, University of Berne, Freiestrasse 3, 3012 Berne, Switzerland*

[2]*Paul-Scherrer-Institut CH-5232 Villigen PSI Switzerland*

**Corresponding author*

α-Tocopherol transfer protein (α-TTP) is a liver protein responsible for the selective retention of α-tocopherol from dietary vitamin E, which is a mixture of α, β, γ, and δ-tocopherols and the corresponding tocotrienols. The α-TTP-mediated transfer of α-tocopherol into nascent VLDL is the major determinant of plasma α-tocopherol levels in humans. Mutations in the α-TTP gene have been detected in patients suffering from low plasma α-tocopherol and ataxia with isolated vitamin E deficiency (AVED).

The crystal structure of α-TTP reveals two conformations. In its closed tocopherol-charged form, a mobile helical surface segment seals the hydrophobic binding pocket. In the presence of detergents, an open conformation is observed, which probably represents the membrane-bound form. The selectivity of α-TTP for RRR-α-tocopherol is explained from the van der Waals contacts occurring in the lipid-binding pocket. Mapping the known mutations leading to AVED onto the crystal structure shows that no mutations occur directly in the binding pocket.

Keywords: ataxia; AVED; crystal structure; tocopherol; vitamin E

Introduction

Vitamin E is a general term for a group of lipophilic compounds, referred to as peroxyl-radical scavengers and chain-breaking antioxidants within biological membranes.[1] Eight different vitamin E forms occur in nature: α, β, γ, and δ-tocopherol having a phytyl tail with three chiral centers in *R*-configuration and α, β, γ, and δ-tocotrienol having an isoprenoid side-chain.[2] Vitamin E deficiency leads to severe degenerative diseases such as ataxia, infertility and Duchène-like muscle degeneration. The connection between these pathological processes and vitamin E is not known in detail but oxidative stress is likely to play a major role.

Absorption studies using vitamin E isotopes have led to the discovery of a remarkable preference for natural RRR-α-tocopherol (RRR-α-T) in healthy adults.[3] The isoforms and stereoisomers of vitamin E are taken up in equal amounts in an unspecific process including emulsification together with food-derived lipids and the subsequent absorption of the formed lipid particles.[4] From the intestine they are transported in chylomicrons and subsequently in remnants to the liver where the cytosolic protein α-TTP is responsible for the stereo-selective transfer of RRR-α-T to VLDL, which is then released into the circulation.[5] *In vitro* as well as *in vivo* assays have shown that α-TTP binds preferentially to the RRR-α-T isomer.[6,7]

Sequence analysis[8] classifies α-TTP as a member of the widespread SEC14-like protein family harboring a characteristic CRAL_TRIO lipid-binding domain.[9] Other members of this family include phosphatidylinositol/phosphatidylcholine transfer protein (SEC14) from *Saccharomyces cerevisiae*,[10] cellular retinaldehyde binding protein (CRALBP)[11] and supernatant protein factor (SPF).[12] All these proteins appear to mediate the intracellular distribution of specific lipids through the aqueous environment by a common mechanism.[13]

The prominent role of α-TTP as carrier of food-derived RRR-α-T has meanwhile been documented in numerous studies.[14] Its importance in maintaining normal plasma α-tocopherol concentrations has been confirmed by analyzing mutations in the

Abbreviations used: α-TTP, α-tocopherol transfer protein; α-T, α-tocopherol; AVED, ataxia with isolated vitamin E deficiency.

E-mail address of the corresponding author: achim.stocker@ibc.unibe.ch

gene of α-TTP in patients suffering from ataxia with vitamin E deficiency (AVED).[15]

Besides high expression rates of α-TTP in the liver, the mammalian brain seems to be able to express its own α-TTP. Accordingly, the neurological phenotype of α-TTP$^{-/-}$ mice has been found to be even more severe and shows an earlier onset than that of wild-type mice when maintained on a α-T-deficient diet,[16] the severe phenotype being unable to walk straight forward. Moreover, a uterine form of α-TTP has been reported to be essential for embryogenesis by supplying the labyrinth region of the placenta with RRR-α-T during development.[17] Both tissues are known to be exposed to high rates of oxidative stress and therefore seem to be specifically protected by α-TTP-mediated tocopherol delivery.

Here we present the crystal structures of a closed "carrier" conformation and an open "membrane-docking" conformation of human α-TTP bound to its physiological ligand RRR-α-T and to the detergent Triton X-100, respectively. This analysis provides the molecular basis of vitamin E retention. Furthermore, it elaborates a model of lipid transfer and opens a way for the rationalization of mutations leading to AVED.

Results

Overall structure of α-TTP

α-TTP crystallizes in two different space groups corresponding to distinct conformational states of the molecule. In the presence of Triton X-100, crystals belonging to the monoclinic space group $P2_1$ were obtained with two α-TTP molecules per asymmetric unit. Addition of RRR-α-T concomitant with removal of Triton X-100 resulted in a tetragonal crystal form containing one molecule per asymmetric unit. The overall conformation of α-TTP is quite similar in both crystal forms with the exception of the helical segment 198–221 (Figure 1).

Our current α-TTP model comprises residues 9–273 in the monoclinic and residues 25–275 in the tetragonal crystal form (Figure 2). In the latter, the N-terminal helix would interfere with a crystal contact and is completely disordered. The protein folds into the prototypical SEC14-like domain structure, which encompasses two highly conserved structural elements, an amino-terminal three-helix coil and a C-terminal CRAL_TRIO lipid-binding domain.[18,19]

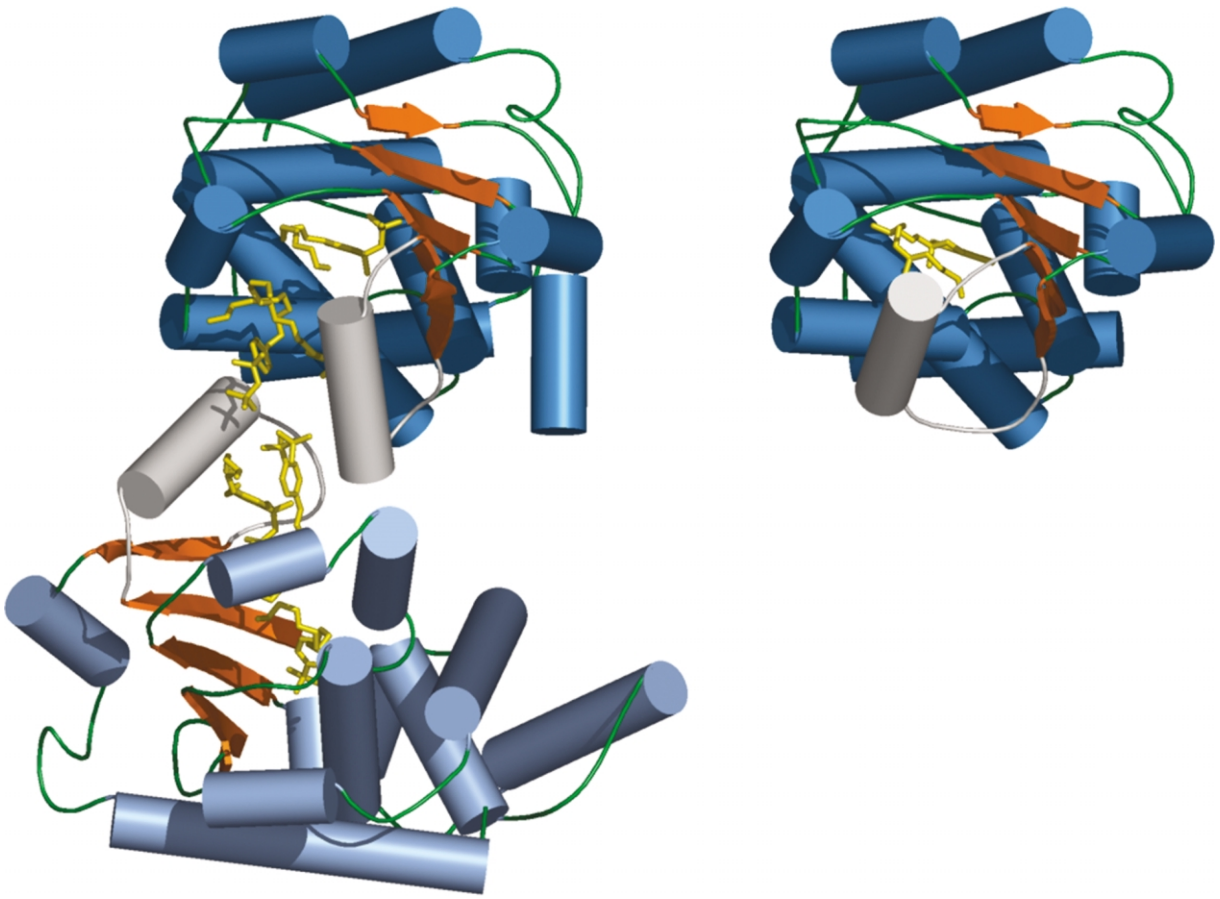

Figure 1. Overview of the open (left) and of the closed (right) conformation of the α-TTP structure. The left picture corresponds to the non-crystallographic dimer. The α-TTP domain backbone is shown in a cartoon representation, with helices colored in blue, β-strands in orange and the lid colored in gray. Triton molecules (left) and RRR-α-tocopherol (right) are shown as stick models with carbons colored yellow. This Figure was prepared using the program PYMOL (Warren Delano, http://www.pymol.org).

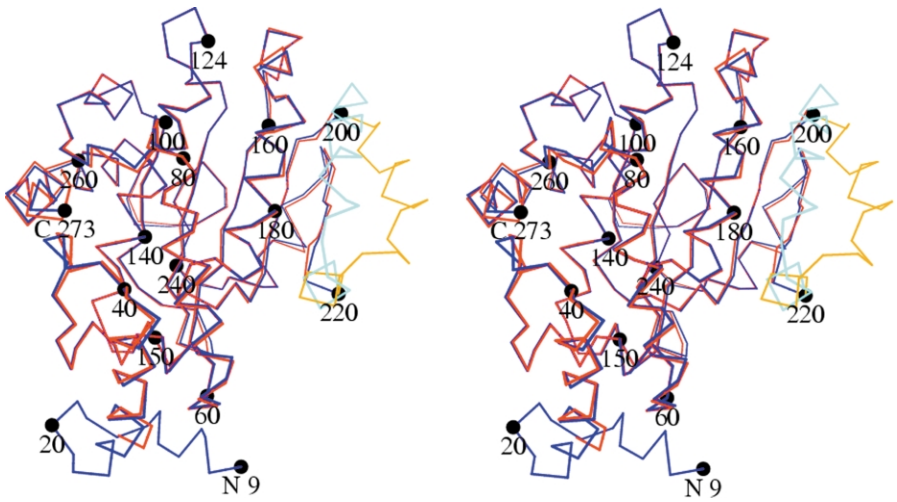

Figure 2. Stereoview of labeled C^{α} traces of the open (blue and cyan) and of the closed (red and orange) conformation of the α-TTP structure.

Functional assignment of the open and the closed conformation of α-TTP

The greatest difference between the two crystal forms occurs in the solvent-exposed residues 198–221, termed "lid". The conformation of this lid affects ligand access to the lipid-binding site. In the RRR-α-T complex the ligand is deeply buried in a hydrophobic pocket, which is closed by the lid. The hydrophobic side of the lid helix lies on the entrance of the pocket while the more polar one faces the solvent (Figure 3).

On the other hand, the Triton complex of α-TTP adopts a conformation with an open lid. The hydrophobic side (residues Ile202, Phe203, Val206 and Ile210) of the lid helix now faces the solvent. This hydrophobic patch is partially covered by a Triton X-100 molecule. A further Triton X-100 molecule is bound within the hydrophobic pocket where it replaces RRR-α-T. The two lids of the NCS-related molecules interact with each other forming the dimer contact area. Interestingly, a similar contact is found in the crystal lattice of the SEC14 structure,[20] which crystallizes in the

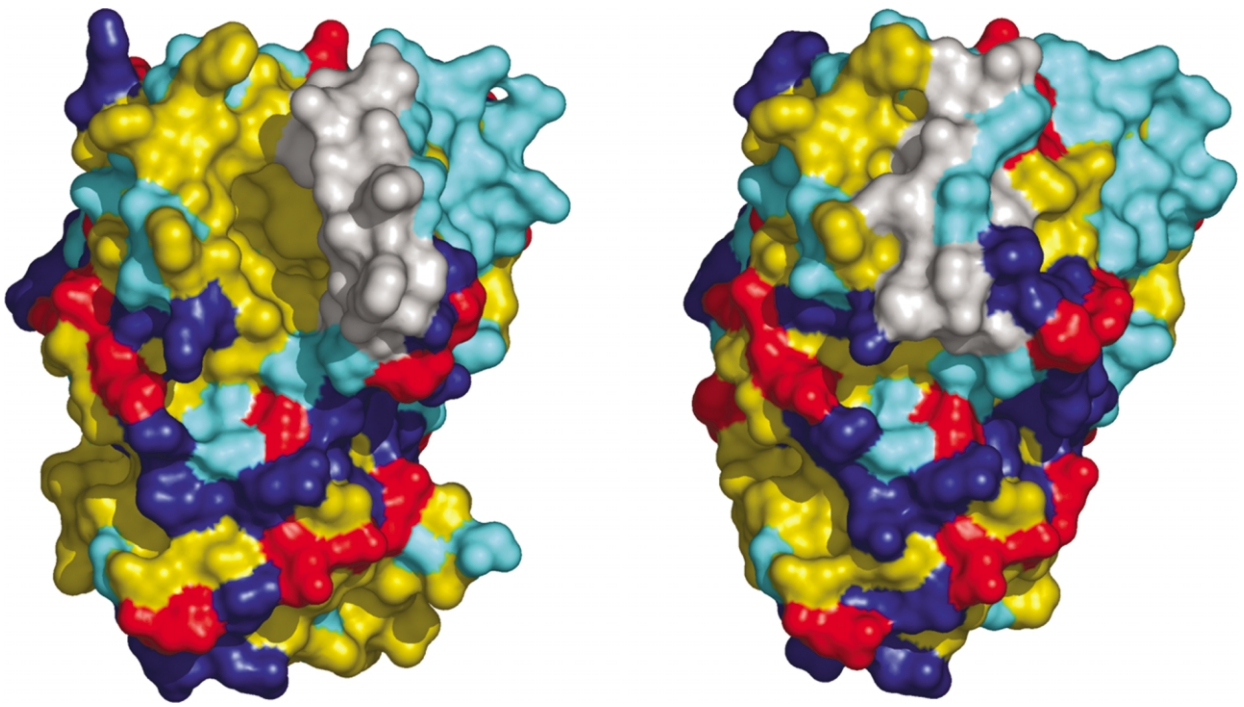

Figure 3. Surface comparison of the open (left) and of the closed (right) conformation of the α-TTP structure. Hydrophobic residues (Ala, Val, Cys, Leu, Ile, Phe, Tyr, Trp, Pro) are colored yellow, basic residues (Arg and Lys) are colored blue, acidic amino acids (Glu and Asp) are red, polar residues (Asn, Gln, Ser, Thr, Gly) are shown in cyan. The hydrophobic key residues of the mobile lipid-exchange loop (residues 198–221) are shown in light gray.

presence of β-octylglucoside in an open conformation as well. The rotation of the lid by about 80° against the plane of the beta-sheet causes a shift of about 14 Å. This large conformational change at the entrance of the cavity contrasts with the absence of significant changes in the rest of the molecule.

The RRR-α-T binding site

The ligand-binding pocket of α-TTP is mostly lined with hydrophobic amino acid side-chains defining a cavity (program VOIDOO)[21] (Figure 4). The chromanol moiety of RRR-α-T is mostly surrounded by hydrophobic residues with the exception of Ser136, Ser140 and three water molecules. One of these connects the tocopherol phenolic hydroxyl group in *para* with the backbone carbonyl group of Val182 through a hydrogen bond. Several water molecules are lined up in a hydrophilic tunnel giving access to the bulk solvent.

The aromatic methyl group in the 5 position of the chromanol moiety fits snugly into a niche formed by the side-chains of residues Ile194, Val191, Ile154 and Leu183, the latter two being in van der Waals contact, with a distance of about 3.6 Å. On the other side of the chromanol ring the two aromatic methyl groups in the 7 and 8 position make contacts to Phe187, Phe133 and Leu137.

The position and geometry of the pyran half-chair of the chromanol ring determine the relative positions of the substituents at the stereocenter in the 2 position with the axial methyl group protruding into an indent of the cavity formed by residues Phe133, Val182 and Ile179 (Figure 4B). The prenyl side-chain is bent into a U-turn involving both stereocenters at the 4′ and at the 8′ position.

Discussion

The structural basis of RRR-α-T selectivity

In vitro tocopherol-transfer studies comparing vitamin E derivatives by Hosomi *et al*. uncovered a preference of α-TTP for RRR-α-T (100%) relative to RRR-β-T (38%), RRR-γ-T (9%) and RRR-δ-T (2%).[6] Of these four naturally occurring analogs, RRR-β-T is found in negligible amounts in food, while RRR-δ-T, RRR-α-T and RRR-γ-T are abundant in different ratios in most edible oils.[22] RRR-γ-T lacks one aromatic methyl group in the 5 position and should therefore fit into the cavity as well (Figure 4). However, the absence of one methyl group reduces the surface available for hydrophobic interactions and diminishes the packing density. Studies by Fersht and co-workers derived an average penalty of 1.3(±0.5) kcal/mol for the removal of a single methylene group from

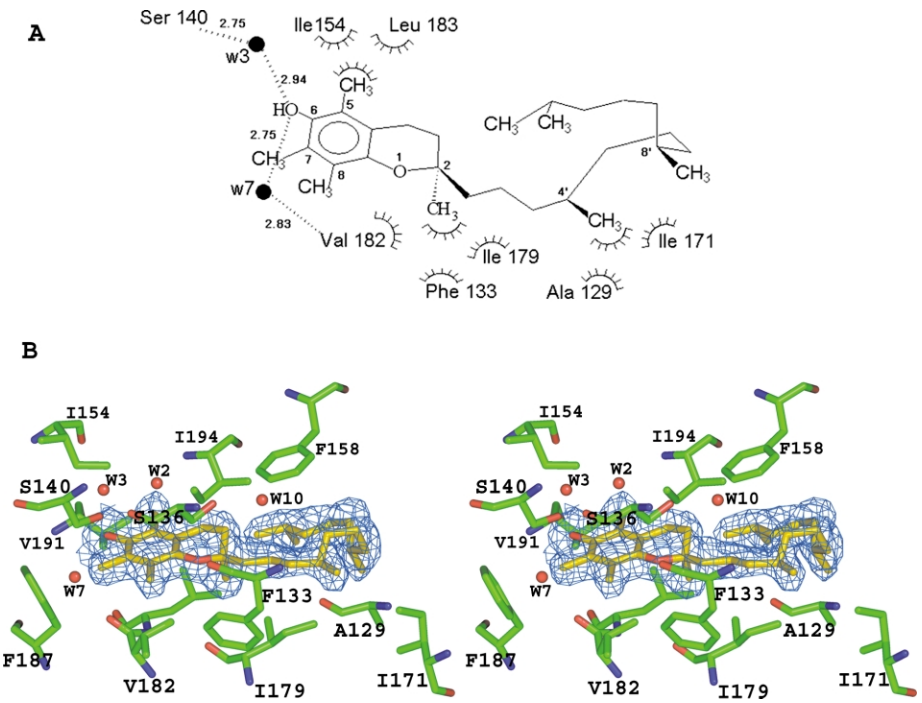

Figure 4. A, Schematic drawing of the interactions between RRR-α-T and the residues within the tocopherol-binding pocket. Possible hydrogen bonds and short contacts are shown with broken lines, and van der Waals contacts are indicated by arcs. This diagram was generated using the program LIGPLOT[51]. B, Stereo figure of the ligand-binding pocket of α-TTP with electron density of bound RRR-α-tocopherol. Shown is a $2F_o - F_c$ density map contoured at 1.0σ above the mean. The map was computed before the ligand was included in the model. RRR-α-tocopherol is depicted as a stick model in dark gray, internal water molecules as black balls, residues within van der Waals distance to the tocopherol molecule in gray.

the hydrophobic main core of chymotrypsin inhibitor 2.[23] Taking this number as a rough guide for the removal of a methyl group from the hydrophobic cavity of α-TTP, the binding ratio $K^{\gamma-T}/K^{\alpha-T}$ is computed as 8.3 ± 6.7 at 310 K. This estimate fits the experimentally determined tenfold reduction in RRR-γ-T binding;[6] of course the error is large due to the varying extent of hydrophobic contacts of a methyl group, which is reflected in the large uncertainty of the figure given by Fersht and co-workers. In the case of RRR-δ-T where an additional methyl group is missing in the 7 position the computed ratio of $K^{\delta-T}/K^{\alpha-T}$ equals 92, a value that correlates reasonably well with the experimentally observed 50-fold reduction in binding,[6] considering again the large error.

In vivo and *in vitro* experiments using eight individual stereoisomers of α-tocopherol have shown that α-TTP possesses stereoselectivity towards *R*-configuration in the 2 position of the chromanol ring.[5,24,25] The synthetic SRR-diastereomer of α-T exhibits a ten times lower affinity for α-TTP than its natural RRR-counterpart,[6] most probably due to a loss of the packing interactions described above (see Figure 4B). The stereocenters in the 4′ and 8′ position of the side-chain were reported to be of minor importance for binding,[26,27] which is attributable to fewer packing restraints and phytyl chain flexibility.

The mechanism of tocopherol transfer

Predictions concerning the transfer mechanism have been based on two main considerations: (i) the transfer protein has to accomplish physical contact with the membrane in a reversible way; and (ii) conformational changes at the protein surface mediate the ligand exchange reaction between the hydrophobic cavity of the protein and the acyl chain environment of the bilayer. These points can now be addressed by the two conformations observed in our crystal structures.

In the closed conformation a large hydrophobic area (Phe203, Val 206, Phe207, Ile210 and Leu214) of the lid is in direct contact with the side-chain of RRR-α-T. Opening of the lid shifts these residues towards the exterior, e.g. to the membrane surface or to the dimer interface in the monoclinic crystal form, establishing new hydrophobic contacts with lipids/detergents or hydrophobic surfaces. Bound tocopherol is then released into the membrane or, *vice versa*, is shuffled into the empty or water-filled binding pocket by lid closure. Water molecules in the cavity, if present, are probably squeezed out through a tunnel connecting the rear of the pocket with the hydrophilic solvent. Well-defined water molecules are visible at the entrance and within the tunnel. The closed lid exposes a more polar face to the solvent and the charged carrier–ligand complex can leave the membrane.

This mechanism, i.e. the presence of a membrane-bound open conformation of the carrier protein where a hydrophobic lid is inserted into the lipid bilayer, followed by transport in a closed conformation of the protein, has been described for the non-homologous phosphatidylinositol transfer protein α.[28,29] The presence of detergents/lipids favors the open conformation also in this case, as well as for SEC14 as mentioned above. Furthermore, similar conformational changes have been observed in lipases, another class of proteins dealing with lipid–water interfaces. The lid comprises an α-helical structure in all cases.[28,30]

The molecular basis of AVED

Several mutations of the human α-TTP gene have been reported to cause vitamin E deficiency, ataxia and retinitis pigmentosa.[15,31,32] The AVED syndrome is characterized by deficient plasma vitamin E and by a progressive peripheral neuropathy with a specific dying back of the larger caliber axons and the sensory neurons, which finally results in ataxia.[33] The linkage of the AVED syndrome to mutations in the α-TTP gene has been confirmed by the production of α-TTP knockout mice exhibiting extremely low RRR-α-T levels and the characteristic neurological disorder.[16]

In humans a striking correlation between the type of mutation, the degree of tocopherol depletion and the severity of the disease has been described.[34] Mild changes in phenotypes are observed in the cases of missense mutations (R192H, H101Q) causing substitutions in non- or semiconserved amino acids. Patients bearing these mutations seem to produce a partially functional protein, which allows them to incorporate RRR-α-T into plasma at reduced rates, leading to a late onset of the disease.[35] Substitutions of highly conserved amino acids, e.g. R59W, E141K and R221W, are associated with the severe, early onset form of AVED disease. The severe form is also observed in cases of protein truncations deriving from frame-shift mutations, mutations affecting intron/exon boundaries and the nonsense mutation R134X. The most abundant truncation mutation has been found in 17 unrelated families with severe AVED, where one base-pair is deleted from position 744 (744delA).[36] The resulting frame-shift leads to the replacement of the last 30 amino acid residues by an aberrant 14 amino acid residue peptide affecting the C-terminal helix (residues 252–272), which extends behind the β-sheet floor of the hydrophobic pocket (Figure 2). In SEC14, the missense mutation G266D, which occurs in this region, renders the protein thermolabile for phospholipid transfer activity *in vitro* and *in vivo* by destabilizing the hydrophobic pocket.[10]

As shown in Figure 5, the missense mutation E141K in α-TTP disrupts the hydrogen bond between the highly conserved E141 on helix 9 (residues 129–143) and Y73. This helix is a central building block of the CRAL_TRIO fold forming one wall of the tocopherol-binding cavity. The presence of a positive charge and the lack of a hydrogen bond in the E141K mutation are

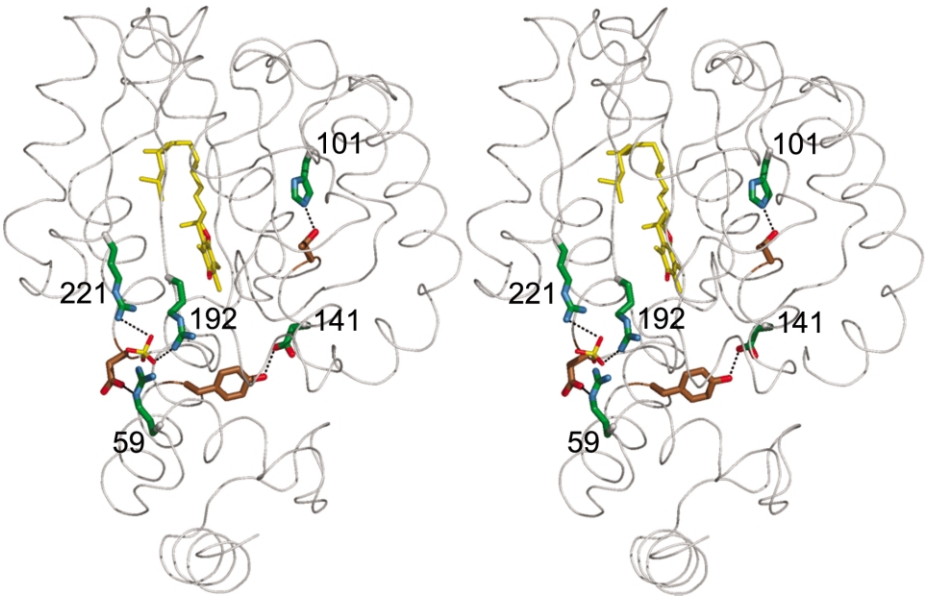

Figure 5. AVED associated mutations in α-TTP. The clinically characterized mutations are mapped onto the three-dimensional structure. Residues that are mutated are shown in green color and carry a label, the interacting amino acid residues described in the text are shown in brown color without label.

sufficient to cause severe AVED, probably by destabilizing the CRAL_TRIO fold. Interestingly, on the opposite site of helix 9 a second hydrogen bond between T139 and the semi-conserved H101 is involved in the missense mutation H101Q (Figure 5). The replacement of histidine by glutamine may not completely abolish the hydrogen bond with T139 and thus exhibits less severe phenotypes than the E141K mutation.[37]

Another set of AVED-associated mutations occurs in a conspicuous cluster of arginine residues, namely R59W, R221W and R192H. These three arginine residues are located on a surface patch that is highly positively charged. Besides these three arginine residues there are further positively charged amino acid residues in the spatial neighborhood, namely R57, R68, R151, K155, K190 and K217. A sulfate ion originating from the crystallization buffer in the tetragonal crystal form is coordinated to K217, R221, K190 and R192. These residues surround the exit of the water-filled tunnel mentioned above, which connects the cavity with the bulk solvent. In two of the missense mutations, namely R59W and R221W, a highly conserved arginine residue is replaced by a hydrophobic tryptophan, while in the case of the R192H mutation the semi-conserved R192 is replaced by a residue of intermediate polarity. The first two mutations are associated with the severe form of AVED, the latter one with a milder pathology. The consequences of the arginine to tryptophan mutations are the disappearance of a positive charge and the placement of a hydrophobic group on the surface. In addition, a salt bridge to D185 is lost in the R59W mutation. The placement of a hydrophobic group on the surface could cause the formation of protein aggregates while the loss of a salt bridge would be expected to destabilize the protein fold. One could also speculate that the positive charge on the surface aids docking to the negatively charged headgroups of the membrane lipids. Interestingly, the K239A missense mutation in SEC14 completely abolishes phosphatidylinositol transfer activity *in vitro*.[38] This residue is conserved in all SEC14 homologs and corresponds to R221 in α-TTP. SEC14 possesses a similar cluster of positively charged residues on this surface segment, namely R63, R65, K66, R119 and K239.

Concluding remarks

Our structural data show that the specificity for RRR-α-T is governed by the packing density within the lipid-binding pocket and can be semi-quantitatively explained. Two different conformations of α-TTP are observed, which can be assigned to the membrane-bound form and the carrier state of the molecule, opening a detailed view on the lipid-exchange mechanism. This mechanism seems to be a general feature of proteins dealing with lipids.

Mutations in the α-TTP gene cause protein malfunction, low plasma RRR-α-T levels, and subsequently the characteristic AVED.[16,35] This severe neurological disorder is observed in cases of protein truncations deriving from frame-shift mutations, mutations affecting intron/exon boundaries and missense mutations. Unexpectedly, none of the known missense mutations of the α-TTP gene affects the lipid-binding pocket or the lid. It may thus be assumed that mutations that are too prohibitive for tocopherol binding are strongly counter-selected, presumably for viability reasons.

Materials and Methods

Protein expression and purification

All analytical grade chemicals were obtained from SIGMA (Buchs, Switzerland). The N-terminal $(His)_6$-tagged α-TTP expression construct was made by cloning the PCR product derived from a human cDNA library into the *Nde*I and *Xho*I sites of the pET-28a vector (Stratagene) using the primers 5′-GGGAATTC CATATGGCAGAGGCGCGATCCCAG-3′ and 5′-CCG CTCGAGTCATTGAATGCTCTCAGAAATGC-3′. *Escherichia coli* BL21(DE3) STAR cells (Invitrogen, Carlsbad) were grown at 25 °C to an $A_{600\,nm}$ of 0.5 and then induced with 1 mM isopropyl-thiogalactopyranoside (IPTG) for 15 hours. Harvested cells were disrupted twice in a French press. α-TTP was purified on 10 ml of Ni-NTA SUPERFLOW (Qiagen, Basel, Switzerland) according to the manufacturer's instructions. The $(His)_6$-tag was cleaved by thrombin digestion (Amersham, Dübendorf, Switzerland) at 4 °C overnight. The protein concentration was determined by the microbiuret method.[39] Typical yields were 0.6 mg/l of pure α-TTP. Higher yields of 8 mg/l were obtained by adding 1% (w/v) Triton X-100 to the disrupted cells and stirring the suspension for 40 minutes at room temperature. After purification on Ni-NTA, the eluate was adjusted to 0.2% (w/v) Triton X-100 and then concentrated by Centriprep-10 (Millipore, Volketswil, Switzerland) to 20 mg/ml. The protein was loaded onto a Superdex 200 column (Amersham) in GPC buffer (20 mM Tris, 100 mM NaCl, 2 mM EDTA, 2 mM DTT, pH 8.0) containing 0.05% (w/v) Triton X-100. One major peak representing the α-TTP fraction was pooled and concentrated to 20 mg/ml and 0.2% (w/v) Triton X-100. The selenomethionine (SeMet)-labeled α-TTP was prepared by the method of methionine biosynthesis inhibition[40] and purified as the wild-type.

Preparation of the RRR-α-T complex with α-TTP

The ligand complex of RRR-α-T with α-TTP was prepared as described with minor modifications.[41] Briefly, purified α-TTP was diluted in 1.5 l of Tris buffer (10 mM, pH 8.5) to a final concentration of 1 μM and tocopherol was added at a 50-fold molar excess from a stock solution of 160 μM RRR-α-T and 100 μM Triton X-100. The diluted protein solution was stirred at 37 °C for one hour and then loaded at 4 °C onto a column containing 10 ml of High Q (Amersham, Dübendorf, Switzerland). After washing with ten volumes the protein was eluted with 20 ml of Tris–NaCl buffer (10 mM Tris, 1 M NaCl, pH 8.5). The eluted protein was transferred into the GPC buffer (20 mM Tris, 100 mM NaCl, 2 mM EDTA, 2 mM DTT, pH 8.0) by Centriprep-10 ultrafiltration and concentrated to 12 mg/ml.

Crystallization and data collection

Monoclinic crystals (Table 1) of α-TTP were obtained at 18 °C by the sitting-drop, vapor-diffusion method. Drops were set up by mixing 1 μl of protein solution

Table 1. Crystallographic statistics

	α-TTP native Triton X100	SeMet-α-TTP Triton X100	α-TTP native RRR-α-T
Crystal parameters	$P2_1$; $a = 45.1$ Å, $b = 113.8$ Å, $c = 67.4$ Å, $\beta = 98.9°$ two molecules/a.s.u[a]	$P2_1$; $a = 45.4$ Å, $b = 113.5$ Å, $c = 67.5$ Å, $\beta = 99.1°$ two molecules/a.s.u	$P4_12_12$; $a = b = 77.7$ Å, $c = 128.2$ Å. one molecule/a.s.u
Data collection (XDS)			
Wavelength (Å)	0.9791	0.9791	1.1407
No. crystals	1	1	1
Resolution range (Å) (outer shell)	30–1.88 (1.90–1.88)	20–2.30 (2.35–2.30)	20–1.95 (1.98–1.95)
No. observations	345,927	346,225[b]	317,025
No. unique reflections	54,206	58,647[b]	29,375
Completeness (%)[c]	99.3 (93.1)	99.3 (92.5)	99.7 (97.7)
R_{sym}[d]	0.051 (0.443)	0.090 (0.271)	0.062 (0.559)
$I/\sigma(I)$	20.2 (3.2)	12.7 (6.3)	22.8 (3.5)
FOM[e]SAD/solvent flattened		0.32/0.57	
Refinement (REFMAC)			
Resolution range (Å)	30–1.88	–	20–1.95
No. reflections working set	51,495	–	27,963
No. reflections test set	2711	–	1472
No. atoms total	4924	–	2208
Protein	4289		2052
Lipid	150[f]		31[g]
Water molecules	294		125
Sulfate ions	0		2
R/R-free(%)	19.5/22.6		19.0/22.7
RMS bonds (Å)	0.010		0.012
RMS angles (deg.)	1.3		1.3

[a] Asymmetric unit.
[b] Friedel pairs were treated as different reflections.
[c] $R_{sym} = \Sigma_{hkl}\Sigma_j|I(hkl;j) - \langle I(hkl)\rangle|/(\Sigma_{hkl}\Sigma_j\langle I(hkl)\rangle)$ where $I(hkl;j)$ is the jth measurement of the intensity of the unique reflection (hkl) and $\langle I(hkl)\rangle$ is the mean over all symmetry-related measurements.
[d] The values in parentheses of completeness, R_{sym} and $I/\sigma(I)$ correspond to the outermost resolution shell.
[e] Figure-of-merit as computed by SOLVE/RESOLVE.
[f] Six Triton X-100 molecules.
[g] One RRR-α-tocopherol molecule.

(18 mg/ml) with 1 μl of reservoir solution (5% (w/v) PEG 6000, 0.1 M Hepes (pH 7.5), 15% (v/v) MPD) and equilibrated against 100 μl reservoir solution at 18 °C. Crystals were observed after ten hours and grew to an average size of 0.25 mm × 0.07 mm × 0.015 mm. Isomorphous crystals of the SeMet-labeled protein were obtained by mixing 1 μl of protein solution (16 mg/ml) with 3 μl of reservoir solution (2.5% (w/v) PEG 2000 MME, 0.1 M Hepes (pH 7.5), 10% (v/v) MPD). Crystals of the RRR-α-T complex of α-TTP were obtained by mixing 1 μl of protein–tocopherol complex solution (12 mg/ml) with 1 μl of reservoir solution (12% (w/v) PEG 6000, 0.1 M sodium citrate (pH 5.6), 0.1 M $LiSO_4$). Tetragonal crystals were observed after two weeks and grew to an average size of 0.05 mm × 0.05 mm × 0.05 mm. Before data collection crystals were flash-cooled in a nitrogen stream at 110 K after raising the MPD concentration of the crystallization solution to 25% (w/v). Data were collected at the SLS synchrotron beamline X06SA (PSI Villigen) at 100 K, employing a MAR-165 CCD (MAR X-ray-research, Hamburg, Germany) detector. Two passes were made to collect high-resolution and overloaded low-resolution reflections. The crystal-to-detector distances varied between 160 mm and 180 mm for selenomethionine derivatives and between 120 mm and 140 mm for the native and tocopherol complex data set. Oscillation angles varied between 1 and 2° per frame, exposure times ranged from one to three seconds. Data were integrated and scaled with XDS[42,43] (Table 1).

Structure solution and refinement

The structure was solved by SAD using SeMet-labeled protein and the monoclinic crystal form which was available first. Six out of eight expected selenium positions were determined using Shake-and-Bake version 2.1,[44] phases were computed using SOLVE 2.01[45] and RESOLVE.[46] Further density modification, phase extension and automatic model building was done by ArpWarp[47] using the native monoclinic data set. Refinement was effected using REFMAC,[48] for model rebuilding the program O was used.[49] Non-crystallographic symmetry restraints were adjusted to give the lowest *R*-free value. Further details are given in Table 1.

The structure of the α-RRR-T complex was determined by molecular replacement using CNS.[50] Clear density for the bound α-RRR-T was visible from the beginning. Refinement statistics are given in Table 1.

Protein Data Bank accession codes

Coordinates of both structures have been deposited in the RCSB Protein Data Bank with ID codes 1oip and 1oiz.

Acknowledgements

This work has been supported by the University of Berne, Switzerland, the Kontaktgruppe für Forschungsfragen of the Basel industry and the Berner Hochschulstiftung. The help of all the staff at the Swiss Light Source in Villigen is highly appreciated.

References

1. Burton, G. W., Joyce, A. & Ingold, K. U. (1983). Is vitamin E the only lipid-soluble, chain-breaking antioxidant in human blood plasma and erythrocyte membranes? *Arch. Biochem. Biophys.* **221**, 281–290.
2. IUPAC-IUB Joint Commission on Biochemical Nomenclature (JCBN) (1982). Nomenclature of tocopherols and related compounds. Recommendations 1981. *Eur. J. Biochem.* **123**, 473–475.
3. Burton, G. W., Traber, M. G., Acuff, R. V., Walters, D. N., Kayden, H., Hughes, L. & Ingold, K. U. (1998). Human plasma and tissue α-tocopherol concentrations in response to supplementation with deuterated natural and synthetic vitamin E. *Am. J. Clin. Nutr.* **67**, 669–684.
4. Gallo-Torres, H. E. (1970). Obligatory role of bile for the intestinal absorption of vitamin E. *Lipids*, **5**, 379–384.
5. Traber, M. G., Sokol, R. J., Burton, G. W., Ingold, K. U., Papas, A. M., Huffaker, J. E. & Kayden, H. J. (1990). Impaired ability of patients with familial isolated vitamin E deficiency to incorporate alpha-tocopherol into lipoproteins secreted by the liver. *J. Clin. Invest.* **85**, 397–407.
6. Hosomi, A., Arita, M., Sato, Y., Kiyose, C., Ueda, T., Igarashi, O. *et al.* (1997). Affinity for alpha-tocopherol transfer protein as a determinant of the biological activities of vitamin E analogs. *FEBS Letters*, **409**, 105–108.
7. Ingold, K. U., Burton, G. W., Foster, D. O., Hughes, L., Lindsay, D. A. & Webb, A. (1987). Biokinetics of and discrimination between dietary RRR- and SRR-α-tocopherols in the male rat. *Lipids*, **22**, 163–172.
8. Arita, M., Sato, Y., Miyata, A., Tanabe, T., Takahashi, E., Kayden, H. J. *et al.* (1995). Human alpha-tocopherol transfer protein: cDNA cloning, expression and chromosomal localization. *Biochem. J.* **306**, 437–443.
9. Kalikin, L. M., Bugeaud, E. M., Palmbos, P. L., Lyons, R. H., Jr & Petty, E. M. (2001). Genomic characterization of human SEC14L1 splice variants within a 17q25 candidate tumor suppressor gene region and identification of an unrelated embedded expressed sequence tag. *Mamm. Genome*, **12**, 925–929.
10. Bankaitis, V. A., Aitken, J. R., Cleves, A. E. & Dowhan, W. (1990). An essential role for a phospholipid transfer protein in yeast Golgi function. *Nature*, **347**, 561–562.
11. Intres, R., Goldflam, S., Cook, J. R. & Crabb, J. W. (1994). Molecular cloning and structural analysis of the human gene encoding cellular retinaldehyde-binding protein. *J. Biol. Chem.* **269**, 25411–25418.
12. Shibata, N., Arita, M., Misaki, Y., Dohmae, N., Takio, K., Ono, T. *et al.* (2001). Supernatant protein factor, which stimulates the conversion of squalene to lanosterol, is a cytosolic squalene transfer protein and enhances cholesterol biosynthesis. *Proc. Natl Acad. Sci. USA*, **98**, 2244–2249.
13. Aravind, L., Neuwald, A. F. & Ponting, C. P. (1999). Sec14p-like domains in NF1 and Dbl-like proteins indicate lipid regulation of Ras and Rho signaling. *Curr. Biol.* **9**, R195–R197.
14. Traber, M. G. & Arai, H. (1999). Molecular mechanisms of vitamin E transport. *Annu. Rev. Nutr.* **19**, 343–355.
15. Ouahchi, K., Arita, M., Kayden, H., Hentati, F., Ben Hamida, M., Sokol, R. *et al.* (1995). Ataxia with isolated vitamin E deficiency is caused by mutations in

the alpha-tocopherol transfer protein. *Nature Genet.* **9**, 141–145.
16. Yokota, T., Igarashi, K., Uchihara, T., Jishage, K., Tomita, H., Inaba, A. *et al.* (2001). Delayed-onset ataxia in mice lacking alpha-tocopherol transfer protein: model for neuronal degeneration caused by chronic oxidative stress. *Proc. Natl Acad. Sci. USA*, **98**, 15185–15190.
17. Jishage, K., Arita, M., Igarashi, K., Iwata, T., Watanabe, M., Ogawa, M. *et al.* (2001). Alpha-tocopherol transfer protein is important for the normal development of placental labyrinthine trophoblasts in mice. *J. Biol. Chem.* **276**, 1669–1672.
18. Zimmer, S., Stocker, A., Sarbolouki, M. N., Spycher, S. E., Sassoon, J. & Azzi, A. (2000). A novel human tocopherol-associated protein: cloning, *in vitro* expression, and characterization. *J. Biol. Chem.* **275**, 25672–25680.
19. Stocker, A., Tomizaki, T., Schulze-Briese, C. & Baumann, U. (2002). Crystal structure of the human supernatant protein factor. *Structure (Camb.)*, **10**, 1533–1540.
20. Sha, B., Phillips, S. E., Bankaitis, V. A. & Luo, M. (1998). Crystal structure of the *Saccharomyces cerevisiae* phosphatidylinositol-transfer protein. *Nature*, **391**, 506–510.
21. Kleywegt, G. J. & Jones, T. A. (1994). Detection, delineation, measurement and display of cavities in macromolecular structures. *Acta Crystallog. sect. D*, **50**, 178–185.
22. Lehmann, J., Martin, H. L., Lashley, E. L., Marshall, M. W. & Judd, J. T. (1986). Vitamin E in foods from high and low linoleic acid diets. *J. Am. Dietet. Assoc.* **86**, 1208–1216.
23. Otzen, D. E., Rheinnecker, M. & Fersht, A. R. (1995). Structural factors contributing to the hydrophobic effect: the partly exposed hydrophobic minicore in chymotrypsin inhibitor 2. *Biochemistry*, **34**, 13051–13058.
24. Traber, M. G., Burton, G. W., Ingold, K. U. & Kayden, H. J. (1990). RRR- and SRR-α-tocopherols are secreted without discrimination in human chylomicrons, but RRR-α-tocopherol is preferentially secreted in very low density lipoproteins. *J. Lipid Res.* **31**, 675–685.
25. Traber, M. G., Rudel, L. L., Burton, G. W., Hughes, L., Ingold, K. U. & Kayden, H. J. (1990). Nascent VLDL from liver perfusions of cynomolgus monkeys are preferentially enriched in RRR- compared with SRR-α-tocopherol: studies using deuterated tocopherols. *J. Lipid Res.* **31**, 687–694.
26. Weiser, H. & Vecchi, M. (1982). Stereoisomers of α-tocopheryl acetate II. Biopotencies of all eight stereoisomers, individually or in mixtures, as determined by rat resorption-gestation tests. *Int. J. Vitam. Nutr. Res.* **52**, 351–370.
27. Weiser, H., Riss, G. & Kormann, A. W. (1996). Biodiscrimination of the eight α-tocopherol stereoisomers results in preferential accumulation of the four 2R forms in tissues and plasma of rats. *J. Nutr.* **126**, 2539–2549.
28. Schouten, A., Agianian, B., Westerman, J., Kroon, J., Wirtz, K. W. & Gros, P. (2002). Structure of apo-phosphatidylinositol transfer protein α provides insight into membrane association. *EMBO J.* **21**, 2117–2121.
29. Yoder, M. D., Thomas, L. M., Tremblay, J. M., Oliver, R. L., Yarbrough, L. R. & Helmkamp, G. M., Jr (2001). Structure of a multifunctional protein. Mammalian phosphatidylinositol transfer protein complexed with phosphatidylcholine. *J. Biol. Chem.* **276**, 9246–9252.
30. van Tiel, C. M., Schouten, A., Snoek, G. T., Gros, P. & Wirtz, K. W. (2002). The structure of phosphatidylinositol transfer protein α reveals sites for phospholipid binding and membrane association with major implications for its function. *FEBS Letters*, **531**, 69–73.
31. Yokota, T., Shiojiri, T., Gotoda, T. & Arai, H. (1996). Retinitis pigmentosa and ataxia caused by a mutation in the gene for the α-tocopherol-transfer protein. *N. Engl. J. Med.* **335**, 1770–1771.
32. Yokota, T., Uchihara, T., Kumagai, J., Shiojiri, T., Pang, J. J., Arita, M. *et al.* (2000). Postmortem study of ataxia with retinitis pigmentosa by mutation of the alpha-tocopherol transfer protein gene. *J. Neurol. Neurosurg. Psychiatry*, **68**, 521–525.
33. Harding, A. E. (1993). Clinical features and classification of inherited ataxias. *Advan. Neurol.* **61**, 1–14.
34. Cavalier, L., Ouahchi, K., Kayden, H. J., Di Donato, S., Reutenauer, S., Mande, J. L. & Koenig, M. (1998). Ataxia with isolated vitamin E deficiency: heterogeneity of mutations and phenotypic variability in a large number of families. *Am. J. Hum. Genet.* **62**, 301–310.
35. Gotoda, T., Arita, M., Arai, H., Inoue, K., Yokota, T., Fukuo, Y. *et al.* (1995). Adult-onset spinocerebellar dysfunction caused by a mutation in the gene for the alpha-tocopherol-transfer protein (see comments). *N. Engl. J. Med.* **333**, 1313–1318.
36. Benomar, A., Yahyaoui, M., Meggouh, F., Bouhouche, A., Boutchich, M., Bouslam, N. *et al.* (2002). Clinical comparison between AVED patients with 744 del A mutation and Friedreich ataxia with GAA expansion in 15 Moroccan families. *J. Neurol. Sci.* **198**, 25–29.
37. Yokota, T., Shiojiri, T., Gotoda, T., Arita, M., Arai, H., Ohga, T. *et al.* (1997). Friedreich-like ataxia with retinitis pigmentosa caused by the His101Gln mutation of the alpha-tocopherol transfer protein gene. *Ann. Neurol.* **41**, 826–832.
38. Phillips, S. E., Sha, B., Topalof, L., Xie, Z., Alb, J. G., Klenchin, V. A. *et al.* (1999). Yeast Sec14p deficient in phosphatidylinositol transfer activity is functional *in vivo*. *Mol. Cell*, **4**, 187–197.
39. Goa, J. (1953). A Micro Biuret method for protein determination. Determination of total protein in cerebrospinal fluid. *Scand. J. Clin. Lab. Invest.* **5**, 218–222.
40. Van Duyne, G. D., Standaert, R. F., Karplus, P. A., Schreiber, S. L. & Clardy, J. (1993). Atomic structures of the human immunophilin FKBP-12 complexes with FK506 and rapamycin. *J. Mol. Biol.* **229**, 105–124.
41. Panagabko, C., Morley, S., Neely, S., Lei, H., Manor, D. & Atkinson, J. (2002). Expression and refolding of recombinant human alpha-tocopherol transfer protein capable of specific α-tocopherol binding. *Protein Expr. Purif.* **24**, 395–403.
42. Kabsch, W. (1993). Automatic processing of rotation diffraction data from crystals of initially unknown symmetry and cell constants. *J. Appl. Crystallog.* **26**, 795–800.
43. Kabsch, W. (1988). Evaluation of single crystal X-ray diffraction data from a position sensitive detector. *J. Appl. Crystallog.* **21**, 916–924.
44. Hauptman, H. A. (1997). Shake-and-bake: an algorithm for automatic solution *ab initio* of crystal structures. *Methods Enzymol.* **277**, 3–13.
45. Terwilliger, T. C. & Berendzen, J. (1999). Automated MAD and MIR structure solution. *Acta Crystallog. sect. D*, **55**, 849–861.

46. Terwilliger, T. C. & Berendzen, J. (1999). Discrimination of solvent from protein regions in native Fouriers as a means of evaluating heavy-atom solutions in the MIR and MAD methods. *Acta Crystallog. sect. D*, **55**, 501–505.
47. Perrakis, A., Morris, R. & Lamzin, V. S. (1999). Automated protein model building combined with iterative structure refinement. *Nature Struct. Biol.* **6**, 458–463.
48. Murshudov, G. N., Vagin, A. A. & Dodson, E. J. (1997). Refinement of macromolecular structures by the maximum likelihood method. *Acta Crystallog. sect. D*, **53**, 240–255.
49. Jones, T. A., Zou, J. Y., Cowan, S. W. & Kjeldgaard (1991). Improved methods for building protein models in electron density maps and the location of errors in these models. *Acta Crystallog. sect. A*, **47**, 110–119.
50. Brunger, A. T., Adams, P. D., Clore, G. M., DeLano, W. L., Gros, P., Grosse-Kunstleve, R. W. *et al.* (1998). Crystallography and NMR system: a new software suite for macromolecular structure determination. *Acta Crystallog. sect. D*, **54**, 905–921.
51. Wallace, A. C., Laskowski, R. A. & Thornton, J. M. (1995). LIGPLOT: a program to generate schematic diagrams of protein-ligand interactions. *Protein Eng.* **8**, 127–134.

Edited by R. Huber

(Received 26 March 2003; received in revised form 28 May 2003; accepted 30 May 2003)